

2020-09

# Mobilisation of antimony from microplastics added to coastal sediment

James, E

<http://hdl.handle.net/10026.1/15744>

---

10.1016/j.envpol.2020.114696

Environmental Pollution

Elsevier BV

---

*All content in PEARL is protected by copyright law. Author manuscripts are made available in accordance with publisher policies. Please cite only the published version using the details provided on the item record or document. In the absence of an open licence (e.g. Creative Commons), permissions for further reuse of content should be sought from the publisher or author.*

1  
2  
3  
4  
5  
6  
7  
8  
9  
10  
11  
12  
13  
14  
15  
16  
17  
18  
19  
20  
21  
22  
23  
24  
25  
26  
27  
28

**Mobilisation of antimony from microplastics added to  
coastal sediment**

**Elanor James & Andrew Turner\***

*School of Geography, Earth and Environmental Sciences  
University of Plymouth  
Drake Circus  
Plymouth PL4 8AA  
UK*

\*Corresponding author. Tel: +44 1752 584570; Fax: +44 1752 584710; e-mail:  
aturner@plymouth.ac.uk

*Keywords:* antimony; microplastics; contamination; deposit-feeders; bioaccessibility;  
kinetics

Accepted 28 April 2020  
<https://doi.org/10.1016/j.envpol.2020.114696>

29 **Abstract**

30 Antimony (Sb) widely occurs in plastics as a pigment and reaction residue and  
31 through the use and recycling of electronic material enriched in Sb as a flame  
32 retardant synergist. In this study, clean estuarine sediment has been contaminated by  
33 different microplastics prepared from pre-characterised samples of different types of  
34 plastic (including a rubber) containing a range of Sb concentrations (256 to 47,600  $\mu\text{g}$   
35  $\text{g}^{-1}$ ). Sediment-plastic mixtures in a mass ratio of 100:1 were subject to 6-hour  
36 extractions in seawater and in seawater solutions of a protein (bovine serum albumin;  
37 BSA) and a surfactant (taurocholic acid; TA) that mimic the digestive conditions of  
38 coastal deposit-feeding invertebrates. Most time-courses for Sb mobilisation could be  
39 defined by a second-order diffusion equation, with rate constants ranging from 44.6 to  
40  $0.0216 (\mu\text{g g}^{-1})^{-1} \text{min}^{-1}$ . Bioaccessibilities, defined as maximum extractable  
41 concentrations throughout each time course relative to total Sb content, ranged from <  
42 0.01 % for a polycarbonate impregnated with Sb as a synergist exposed to all  
43 solutions, to > 1 % for acrylonitrile butadiene styrene containing a Sb-based colour  
44 pigment exposed to solutions of BSA and TA and recycled industrial polyethylene  
45 exposed to BSA solution. The potential for Sb to bioaccumulate or elicit a toxic effect  
46 is unknown but it is predicted that communities of deposit-feeders could mobilise  
47 significant quantities of Sb in sediment contaminated by microplastics through  
48 bioturbation and digestion.

49

50 **Keywords:** antimony; plastics; sediment; mobilisation; bioaccessibility

51

52 **Capsule:** Antimony is mobilised from plastics added to sediment by seawater and  
53 solutions of a protein and a surfactant via a diffusion model

54

## 55 **1. Introduction**

56 Antimony and many of its compounds display both acute and chronic toxicity to a  
57 range of organisms (Tschan et al., 2010; Paoli et al., 2013; Yang, 2014; Yang et al.,  
58 2018). In humans, exposure to Sb has been related to respiratory, cardiovascular and  
59 gastrointestinal symptoms and antimony trioxide ( $\text{Sb}_2\text{O}_3$ ) is classified as possibly  
60 carcinogenic (Sundar and Chakravarty, 2010; Tamás, 2016). Antimony is also a  
61 technology-critical element in that it has economic importance to emerging  
62 technologies but is subject to a high supply risk (Nuss and Blengini, 2018). Current  
63 applications of Sb include pigments for colour or colour protection, decolouring and  
64 refining agents in glass, catalysts for polycondensation, synergists for flame  
65 retardants, and alloys in batteries in ammunition, antifriction bearings, cable sheaths  
66 and roofing (Yellishetty et al., 2017).

67

68 Antimony is particularly pervasive in synthetic polymers (including textiles, plastics  
69 and rubbers) (Filella et al., 2020). Here it is used in various pigments, but its principal  
70 application that results in the highest concentrations is as a synergist for halogenated  
71 flame retardants (as  $\text{Sb}_2\text{O}_3$ , the pentoxide,  $\text{Sb}_2\text{O}_5$ , or sodium antimonite,  $\text{Na}_3\text{SbO}_4$ ;  
72 Papazoglou, 2004). The trioxide is also used as a catalyst for the production of  
73 polyethylene terephthalate (PET), including fibrous polyester, and residues of the  
74 compound and other reaction products (including organic-complexes of Sb) remain in  
75 the material after manufacture (Welle and Franz, 2010). Antimony is more widely  
76 dispersed amongst consumer and commercial plastics through the recycling of end-of-  
77 life products. In this respect a particular problem arises when flame-retarded  
78 electronic plastics are recycled into consumer goods in which halogenated compounds  
79 and Sb are neither expected nor desired (Turner and Filella, 2017).

80

81 Concerns over the presence and possible migration of Sb in consumer products, and in  
82 particular plastics, has resulted in guidelines or regulations for the metalloid. In PET  
83 food-contact and storage items, where Sb concentrations are typically a few hundred  
84  $\mu\text{g g}^{-1}$  (Westerhoff et al., 2008), migration into liquids is effectively limited to  $5 \mu\text{g L}^{-1}$   
85 <sup>1</sup> according to EC Directive 2003/40 on natural mineral waters (European  
86 Commission, 2003). Migration into foods is limited to  $40 \mu\text{g}$  per kg of food according  
87 to EU Regulation 10/2011 (European Commission, 2011) and based on the tolerable

88 daily intake of  $6 \mu\text{g kg}^{-1}$  body weight (World Health Organization, 2003). In plastic,  
89 rubber or painted toys, migration of Sb is limited by the amended EC Toy Safety  
90 Directive to between  $11.3$  and  $560 \mu\text{g g}^{-1}$  depending on the characteristics of the  
91 material (based on pliability, size, thickness, brittleness) (European Parliament and  
92 Council of the EU, 2009). Despite concentrations of Sb in flame-retarded electronic  
93 plastics that can exceed several percent by weight (Papazoglou, 2004), the metalloid  
94 is currently not included in the list of substances defined by the original or recast  
95 Restriction on Hazardous Substances (RoHS) Directives (European Parliament and  
96 Council, 2003; 2011). However, the EU regards Sb as a “heavy metal” and defines  
97 waste as “ecotoxic” if heavy metal concentrations exceed certain thresholds  
98 (European Commission, 2018).

99

100 As a result of its widespread use in and contamination of polymers, Sb is predicted to  
101 be commonly encountered in marine litter. X-ray fluorescence (XRF) analysis of  
102 consumer, maritime and industrial plastics collected by hand from the strandlines of  
103 various beaches in south west England has revealed the presence of Sb in up to 50%  
104 of a wide variety of samples of relatively low density (but mainly polyethylene and  
105 polypropylene) (Shaw and Turner, 2019; Turner et al., 2019). However, given that  
106 microplastics buried below the sediment surface, including microfibers, appear to  
107 contain a higher proportion of denser materials like PET (Yu et al., 2018; Zheng et al.,  
108 2019), the overall abundance of Sb in marine litter may be significantly greater.

109

110 In coastal regions where the substrate is contaminated by synthetic polymers  
111 (hereafter referred to as plastics), benthic and infaunal animals may be exposed to  
112 elevated levels of Sb. Of particular significance in this respect are deposit-feeding  
113 invertebrates that non-selectively process large quantities of material through  
114 burrowing, ingestion and egestion. Exposure could increase should quantities of Sb be  
115 mobilised from microplastics through bioturbating activities, and in particular during  
116 digestion. Accordingly, the present study examines the potential for Sb to be released  
117 from plastics via coastal deposit-feeders by incubating preparations of clean sediment  
118 and a range of microplastics in fluids that simulate the invertebrate digestive  
119 environment. Specifically, we use seawater solutions of the protein, bovine serum  
120 albumin (BSA; molecular mass =  $66,400 \text{ g mol}^{-1}$ ), to mimic the complexing capacity

121 of amino acids (Chen and Mayer, 1998), and the vertebrate bile acid surfactant,  
122 taurocholic acid (TA;  $C_{26}H_{44}NO_7SNa$ ; molecular mass =  $537.7 \text{ g mol}^{-1}$ ), as a  
123 surrogate for anionic surfactancy (Voparil and Mayer, 2004).

124

## 125 **2. Materials and methods**

### 126 *2.1. Sourcing and characterisation of plastics*

127 About 50 plastics items sourced from archived litter samples and consumer products  
128 were analysed for total Sb and polymer type according to protocols outlined  
129 elsewhere (Turner et al., 2019). Briefly, Sb was determined on three regions of each  
130 sample by portable XRF spectrometry using a battery-operated Niton XL3t 950 He  
131 GOLDD+ portable XRF. The instrument was operated for a period of 60 seconds in  
132 a “plastics” mode with thickness correction and performance was checked regularly  
133 by analysing a polyethylene reference disk reference (Niton PN 180-619) that  
134 contained Sb at a concentration of  $96 \pm 10 \mu\text{g g}^{-1}$ . Polymer identification on small (<  
135 5 mg) sample offcuts was performed by attenuated total reflectance Fourier-  
136 transform-infrared (ATR-FTIR) spectrometry using a Bruker Vertex 70.

137

138 Based on the analyses above, seven plastics of varying Sb content and polymeric  
139 composition, including one sample of rubber, were selected for use in the extraction  
140 experiments (Table 1). The sample of PET likely contains Sb as catalytic residue  
141 arising from the manufacture of the material, while acrylonitrile butadiene styrene  
142 (ABS) contains Sb as a component of the pigment titanium yellow (CI Pigment  
143 Yellow 53;  $NiO \cdot Sb_2O_3 \cdot 20TiO_2$ , and confirmed by the presence of Ni and Ti in the  
144 XRF spectrum). Polystyrene (PS), polycarbonate (PC) and polyethylene (PE) contain  
145 Sb as a flame retardant synergist in the presence of brominated compounds, and  
146 polyvinyl chloride (PVC) and rubber (R) appear to contain Sb as a synergist in the  
147 presence of chlorinated compounds. Using a stainless steel grater, at least 1 g of each  
148 sample was formulated into microplastic particles (< 1 mm in at least two  
149 dimensions) that were stored in individual polyethylene specimen bags.

150

### 151 *2.2. Sediment sampling and processing*

152 Approximately 1.5 L of surficial, oxic sandy-silty sediment was collected using a  
153 plastic trowel from the lower, intertidal reaches of a protected estuary that is

154 relatively unpolluted with regard to both metals and plastics (Erme, south west  
155 England; 50.3111, -3.9457). On site, the sample was sieved through a 1 mm Nylon  
156 mesh into a plastic bucket. In the laboratory, subsamples of about 250 g were  
157 transferred to a series of clear zip-locked polyethylene bags and stored frozen until  
158 required. The chemical characteristics of the fractionated sediment sample,  
159 determined on freeze-dried aliquots, are given in Table 2. Here, metal concentrations  
160 were determined by inductively coupled plasma-optical emission spectrometry (ICP-  
161 OES) and Sb concentration by inductively coupled plasma-mass spectrometry (ICP-  
162 MS; see below) according to established protocols (Turner, 2019) and following  
163 digestion of triplicate 250 mg aliquots in aqua regia heated to 80 °C for 2 h. Loss on  
164 ignition (LOI) as a proxy for organic matter content was determined by mass loss on  
165 ignition at 500°C for 8 h.

166

### 167 *2.3. Experimental*

168 One-litre solutions that mimic the chemical conditions (amino acid composition and  
169 surfactancy) encountered in the digestive environment of temperate, coastal deposit-  
170 feeding invertebrates were prepared in 0.45 µm-filtered English Channel seawater ( $S$   
171 = 33; pH 7.8) in a series of borosilicate bottles. Specifically, these consisted of 4 g L<sup>-1</sup>  
172 of the protein, BSA (> 96% fraction V; Sigma Aldrich), 4 g L<sup>-1</sup> of TA (taurocholic  
173 acid sodium salt hydrate, 97%+; VWR International), and 4 g L<sup>-1</sup> of BSA plus 4 g L<sup>-1</sup>  
174 TA.

175

176 Experiments were undertaken according to protocols outlined in Jones and Turner  
177 (2010) and Martin and Turner (2019). Thus, bags of sediment were defrosted as  
178 required and aliquots of 25 g (or 18.26 g on a dry weight basis) were weighed into a  
179 series of eight screw-capped 200 mL polyethylene bottles. To seven of the bottles,  
180 250 mg of the different microplastics were added, with the eighth bottle serving as a  
181 plastic-free control. The concentration of plastic in the sediment on a dry weight  
182 basis was, therefore, about 14 g kg<sup>-1</sup>. This is higher than microplastic abundance  
183 reported in contaminated sediments (up to about 130 mg kg<sup>-1</sup>; He et al., 2020) but  
184 was selected in order to allow the ready detection of mobilised Sb.

185

186 One hundred ml of seawater (SW) was pipetted into each bottle before the contents  
187 were agitated on a Stuart SSL1 benchtop orbital shaker set at 150 rpm at room  
188 temperature and in the dark. After 15 min, 30 min, 1 h, 2 h, 4 h, 5 h and 6 h,  
189 subsamples of 5 mL were pipetted into 15 mL polypropylene centrifuge tubes and  
190 centrifuged at 3000 rpm for 10 min before 2-mL supernatants were transferred to  
191 Sterilin tubes, diluted to 10 ml with 2% HNO<sub>3</sub> and stored at 4°C and in the dark  
192 pending analysis. This approach was repeated using seawater solutions of BSA (SW  
193 + BSA), taurocholic acid (SW + TA) and BSA plus taurocholic acid (SW + BSA +  
194 TA).

195

#### 196 *2.4. Analysis of extracts*

197 A ThermoScientific iCAP RQ ICP-MS with a Glass Expansion micromist nebuliser  
198 and cyclonic spray chamber was used to determine Sb concentrations in the diluted  
199 extracts. The instrument was calibrated with a blank and four standards (up to 20 µg  
200 L<sup>-1</sup>) prepared by serial dilution of a LabKings 10000 mg L<sup>-1</sup> Sb standard in 2% HNO<sub>3</sub>.  
201 Radio frequency power was set at 1.5 KW with coolant, nebuliser and auxiliary flows  
202 of 1.4, 1.07 and 0.8 L Ar min<sup>-1</sup> and a replicate ( $n = 3$ ) read time of 10 ms. Detection  
203 limits arising from three standard deviations of blank measurements were between  
204 0.05 and 0.10 µg L<sup>-1</sup> and precision among replicate readings was better than 15% for  
205 mean concentrations above 0.5 µg L<sup>-1</sup> and up to 25% for lower mean concentrations .  
206

### 207 **3. Results and Discussion**

#### 208 *3.1. Antimony concentrations in the plastic-amended sediment samples*

209 Table 3 presents the dry weight concentrations of total Sb in the estuarine sediment  
210 and in sediment amended by the different microplastics defined in Table 1. Note that  
211 in the sediment amendments concentrations are computed from the fractional  
212 contributions of sediment and plastic to total dry mass and the total concentrations of  
213 Sb in the different solids. Thus, mass contamination of coastal sediment by about  
214 1.4% of these plastics results in total Sb concentrations that are orders of magnitude  
215 greater than the Sb content of sediment itself.

216

#### 217 *3.2. Antimony mobilisation kinetics*



218 Figure 1 shows the dry weight normalised concentrations of Sb released from the  
219 sediment and sediment amendments, [Sb], for the different solutions as a function of  
220 time,  $t$ . In some cases, [Sb] increases throughout the incubation (e.g. sediment + R in  
221 SW + BSA) or there is a reduction in [Sb] following a period of rapid increase (e.g.  
222 sediment + PE in SW + BSA). In most cases, however, [Sb] increases over the  
223 experimental period and appears to approach equilibrium. Here, data were modelled  
224 using a second-order diffusion model (Ruby et al., 1992; Martin and Turner, 2019):

225

$$226 \quad 1/([Sb]_e - [Sb]) = 1/[Sb]_e + kt \quad (1)$$

227

228 where  $[Sb]_e$  is the “equilibrium” concentration of the metalloid defined as the highest  
229 concentration reported among the last five data points (i.e.  $t > 120$  min), and  $k$  is a  
230 second-order rate constant of units  $(\mu\text{g g}^{-1})^{-1} \text{min}^{-1}$ . Rate constants were derived from  
231 the slopes of  $(1/([Sb]_e - [Sb]) - 1/[Sb]_e)$  versus  $t$ , provided that linear regressions were  
232 significant ( $p < 0.05$ ), and are given in Table 4 along with values of  $[Sb]_e$ . Where  
233 timed data were more complex or equilibrium was not approached, maximum  
234 measured values of the metalloid,  $[Sb]_{\text{max}}$ , are given in the table.

235

236 For sediment alone, the greatest concentration of Sb mobilised (as  $[Sb]_e$  or  $[Sb]_{\text{max}}$ )  
237 was in SW. Among the samples amended with plastics, however, there was no clear  
238 pattern of mobilisation among the different solutions, with each mobilising the  
239 greatest concentration of Sb from at least one sample. Overall, second-order rate  
240 constants ranged from  $44.6 (\mu\text{g g}^{-1})^{-1} \text{min}^{-1}$  for sediment amended with PS in the  
241 presence of SW + BSA + TA to  $0.0216 (\mu\text{g g}^{-1})^{-1} \text{min}^{-1}$  for sediment amended with PE  
242 in the presence of SW alone.

243

### 244 *3.3. Antimony bioaccessibility*

245 Bioaccessibility may be defined as the fraction of a contaminant that is available for  
246 dissolution in the digestive tract of an organism, and provides an upper-estimate of  
247 bioavailability, or the amount that is able to enter the systemic circulation (Weston  
248 and Mayer, 1998). Upper estimates of the percentage bioaccessibility of Sb in  
249 sediment and sediment amended with plastic to a range of deposit-feeding  
250 invertebrates (i.e. with varying proteins and degrees of surfactancy in their digestive

251 environments) were calculated from  $[Sb]_e$  or  $[Sb]_{max}$  relative to total Sb and are shown  
252 in Table 5. Overall, BA is greatest for sediment alone, where the metalloid is likely  
253 adsorbed to the particles surface and bound in different mineral phases of varying  
254 solubility, with estimates ranging from 0.67 for SW + TA to 2.67 % for SW itself.  
255 Where plastic is present, the highest values of bioaccessibility were observed for  
256 amendments with ABS, PE and R. For ABS, similar values of bioaccessibility were  
257 exhibited for each solution. However, sediment amended with PE exhibits a value that  
258 is greatest by two orders of magnitude when BSA is present without TA, and  
259 sediment amended with R exhibits values that are an order of magnitude greater for  
260 SW and SW + BSA than when TA is present. Among the remaining plastics,  
261 bioaccessibility is lowest overall for PC and greatest for PET.

262

### 263 *3.4. Mechanisms of antimony mobilisation from plastics*

264 The release of ions and molecules from polymers normally proceeds by diffusion  
265 (Nakashami et al., 2016; Town et al., 2018) but very little has been studied in respect  
266 of Sb release from marine plastics. Specifically, as part of a study into metal and  
267 metalloid bioaccessibility in various plastics subject to simulated, acidic avian  
268 digestion, Turner (2018) established that Sb mobilisation from two samples of  
269 micronized polypropylene under simulated avian digestive conditions proceeded via a  
270 pseudo-first-order diffusion process with rate constants of about  $0.05 \text{ h}^{-1}$ .

271

272 Because of human health concerns, a greater body of literature exists regarding the  
273 migration of Sb from polyethylene terephthalate (PET) food-contact plastics that  
274 contain the metalloid as catalytic residue (Haldimann et al., 2007; Rungchang et al.,  
275 2013; Chapa-Martínez et al., 2016). It appears that Sb diffusion is dependent on the  
276 physical and chemical nature of migrating species or compounds, the properties of the  
277 plastic, including crystallinity, polarity and molecular weight, plastic surface area to  
278 solution volume ratio, and the presence of any other additives in the plastic that may  
279 retard or facilitate the diffusion process through, for example, adsorption (Westerhoff  
280 et al., 2008; Haldimann et al., 2013).

281

282 In this study, Sb is likely present as  $Sb_2O_3$  where the metalloid is employed directly  
283 (or introduced through recycling) as a flame retardant synergist (Papazoglou, 2004),  
284 and, additionally, as a series of glycolate complexes in PET as products of the

285 polymerisation process (El-Toufaily et al., 2006); in ABS, however, Sb is present as  
286 part of the complex pigment, titanium yellow. Accordingly, the comparatively rapid  
287 release of Sb from PET can be attributed to the relatively high diffusivity of rather  
288 small organic-complexes of Sb (Welle and Franz, 2010), while for ABS enhanced  
289 mobilisation could be due to the presence of Ti, which, despite its sorptive properties,  
290 has been observed to promote diffusion of Sb in plastic (Haldimann et al., 2013).  
291 Differences between the mobilisation of Sb from other materials can be related to  
292 polymer permeability; for example, published permeation coefficients (for oxygen)  
293 are around  $10^3 \text{ cm}^3 \text{ mm m}^{-2} \text{ d}^{-1} \text{ atm}^{-1}$  for various rubbers but are an order of magnitude  
294 lower for PVC, PS and PC (Keller, 2017).

295

296 Despite these qualitative explanations, however, it is important to bear in mind that  
297 net mobilisation of Sb is also dependent on largely unknown interactions of migrating  
298 species with the sediment surface (e.g. through adsorption) and substances present in  
299 the aqueous medium (e.g. through complexation), and interactions among aqueous  
300 constituents and between these constituents and the sediment surface.

301

### 302 *3.5. Bioaccessibility and mobilisation of Sb in the coastal zone*

303 Antimony is commonly encountered in a wide range of plastics as a flame retardant  
304 synergist (often through the recycling of electronic waste), a pigment and a catalyst,  
305 and is one of the main inorganic residues in polyester fibres (Turner, 2019). Given the  
306 abundance of microplastics in many coastal sediments (up to several thousand  $\text{kg}^{-1}$   
307 have been recorded; Lots et al., 2017; Lo et al., 2018; Wang et al., 2019) these  
308 particles could represent a significant anthropogenic source of Sb in the littoral zone.  
309 For example, 1 kg of the estuarine sediment used in the present study would double its  
310 Sb concentration (to  $0.36 \mu\text{g g}^{-1}$ ) if contaminated by just 3.6 mg of flame-retarded  
311 rubber particles.

312

313 Many invertebrates inhabiting the littoral zone incidentally and non-selectively ingest  
314 microplastics as part of their sedimentary diet (Van Cauwenberghe et al., 2015; Setala  
315 et al., 2016) and are thereby exposed to quantities of additives and residues that, in  
316 some cases, could be considerable. For example, colonies of the deposit-feeding  
317 lugworm, *Arenicola marina*, may actively process up to  $80 \text{ cm}^3$  of sediment per  $\text{m}^2$

318 per day (Kesy et al., 2016) while individual holothurians may ingest-defecate up to 82  
319 kg per year (Renzi et al., 2018). Whether sufficient Sb is bioaccessible and  
320 accumulated to elicit some adverse effect is unknown because the toxicity of the  
321 metalloid in the marine environment is poorly documented. However, the processing  
322 and bioturbation of plastic-contaminated sediment is likely to be critical to the  
323 mobilisation and redistribution of more bioavailable forms of the element (and to  
324 polymer-bound contaminants more generally) in the local interstitial environment and  
325 overlying water column.

326

#### 327 **4. Conclusions**

328 Antimony is a technology-critical element that is commonly present in plastics as an  
329 additive, residue or contaminant. This study has shown that Sb can be partially  
330 mobilised from micronized plastics added to sediment by seawater and solutions  
331 mimicking the digestive chemistry of deposit-feeding invertebrates. Mobilisation  
332 often proceeds via a second-order diffusion model and over a six-hour period can  
333 range from between about 0.01% and 3.5% of total Sb depending on the type of  
334 solution and nature of the plastic. Large communities of deposit-feeders could be  
335 instrumental to the dissolution and mobilisation of the element from sediment  
336 contaminated by microplastic.

337

#### 338 **Acknowledgements**

339 Mr Andy Arnold, Dr Alex Taylor and Dr Andy Fisher (UoP) are thanked for technical  
340 and analytical assistance throughout the study.

341

#### 342 **References**

343 Chapa-Martínez, C.A., Hinojosa-Reyes, L., Hernández-Ramírez, A., Ruiz-Ruiz, E.,  
344 Maya-Treviño, L., Guzmán-Mar, J.L., 2016. An evaluation of the migration of  
345 antimony from polyethylene terephthalate (PET) plastic used for bottled drinking  
346 water, *Sci. Total Environ.* 565 511–518.

347

348 Chen, Z., Mayer, L.M., 1998. Mechanisms of Cu solubilisation during deposit  
349 feeding. *Environmental Science and Technology* 32, 770-775.

350

351 El-Toufaily, F.A., Feix, G., Reichert, K.H., 2006. Mechanistic investigations of  
352 antimony-catalyzed polycondensation in the synthesis of poly(ethylene terephthalate).  
353 Journal of Polymer Science A: 44:1049–1059.  
354

355 European Commission., 2003. Commission Directive 2003/40/EC of 16 May 2003  
356 establishing the list, concentration limits and labelling requirements for the  
357 constituents of natural mineral waters and the conditions for using ozone-enriched  
358 air for the treatment of natural mineral waters and spring waters. Official Journal of  
359 the European Union L126, 34–39.  
360

361 European Commission, 2011. Commission Regulation (EU) No. 10/2011 of 14  
362 January 2011 on plastic materials and articles intended to come into contact with  
363 food. Official Journal of the European Union L12/1.  
364

365 European Commission, 2018. Commission notice on technical guidance on the  
366 classification of waste (2018/C 124/01). Official Journal of the European Union  
367 C124/1.  
368

369 European Parliament and Council, 2003. Directive 2002/95/EC on the restriction of  
370 the use of certain hazardous substances in electrical and electronic equipment. Official  
371 Journal of the European Union L37/19.  
372

373 European Parliament and Council, 2011. Directive 2011/65/EU on the restriction of  
374 the use of certain hazardous substances in electrical and electronic equipment (recast).  
375 Official Journal of the European Union L174/88.  
376

377 European Parliament and Council of the EU, 2009. Directive 2009/48/EC of the  
378 European Parliament and of the Council of 18 June 2009 on the safety of toys.  
379 Official Journal of the European Union L170/1.  
380

381 Filella, M., Hennebert, P., Okkenhaug, G., Turner, A., 2020. Occurrence and fate of  
382 antimony in plastics. Journal of Hazardous Materials 390, 121764.  
383

384 Haldimann, M., Blanc, A., Dudler, V., 2007. Exposure to antimony from polyethylene  
385 terephthalate (PET) trays used in ready-to-eat meals. Food Additives and  
386 Contaminants 24, 860-868.  
387  
388 Haldimann, M., Alt, A., Blanc, A., Brunner, K., Sager, F., Dudler, V., 2013.  
389 Migration of antimony from PET trays into food simulant and food: determination of  
390 Arrhenius parameters and comparison of predicted and measured migration data.  
391 Food Additives and Contaminants A 30, 587-598.  
392  
393 He, B.B., Goonetilleke, A., Ayoko, G.A., Rintoul, L., 2020. Abundance, distribution  
394 patterns, and identification of microplastics in Brisbane River sediments, Australia.  
395 Science of the Total Environment 700, 134467.  
396  
397 Jones, D.E., Turner, A., 2010. Bioaccessibility and mobilisation of copper and zinc in  
398 estuarine sediment contaminated by antifouling paint particles. Estuarine and Coastal  
399 Shelf Science 87, 399-404.  
400  
401 Lo, H.S., Xu, X.Y., Wong, C.Y., Cheung, S.G., 2017. Comparisons of microplastic  
402 pollution between mudflats and sandy beaches in Hong Kong. Environmental  
403 Pollution 236, 208-217.  
404  
405 Lots, F.A.E., Behrens, P., Vijver, M.G., Horton, A.A., Bosker, T., 2017. A large-scale  
406 investigation of microplastic contamination: Abundance and characteristics of  
407 microplastics in European beach sediment. Marine Pollution Bulletin 123, 219-226.  
408  
409 Keller, P.E., 2017. Water Vapor Permeation in Plastics. Pacific Northwest National  
410 Laboratory for the US Department of Energy, Springfield, VA.  
411  
412 Kesy, K., Oberbeckmann, S., Müller, F., Labrenz, M., 2016. Polystyrene influences  
413 bacterial assemblages in *Arenicola marina*-populated aquatic environments *in vitro*.  
414 Environmental Pollution 219, 219-227.  
415  
416 Martin, K., Turner, A., 2019. Mobilization and bioaccessibility of cadmium in coastal  
417 sediment contaminated by microplastics. Marine Pollution Bulletin 146, 940-944.

418

419 Nakashima, E., Isobe, A., Kako, S., Itai, T., Takahashi, S., Guo, X., 2016. The  
420 potential of oceanic transport and onshore leaching of additive-derived lead by marine  
421 macro-plastic debris. *Marine Pollution Bulletin* 107, 333-339.

422

423 Nuss, P., Blengini, G.A., 2018. Towards better monitoring of technology critical  
424 elements in Europe: Coupling of natural and anthropogenic cycles. *Science of the*  
425 *Total Environment* 613, 569-578.

426

427 Paoli, L., Fiorini, E., Munzi, S., Sorbo, S., Basile, A., Loppi, S., 2013. Antimony  
428 toxicity in the lichen *Xanthoria parietina* (L.) Th. Fr. *Chemosphere* 93, 2269-2275.

429

430 Papazoglou, E.S., 2004. Flame retardants for plastics. In: *Handbook of Building*  
431 *Materials for Fire Protection*, Harper, C.A., ed, McGraw-Hill, New York.

432

433 Runchang, S., Numthuam, S., Qui, X.L., Li, Y.J., Satake, T., 2013. Diffusion  
434 coefficient of antimony leaching from polyethylene terephthalate bottles into  
435 beverages. *Journal of Food Engineering* 115, 322-329.

436

437 Renzi, M., Blaskovic, A., Bernardi, G., Russo, G.F., 2018. Plastic litter transfer from  
438 sediments towards marine trophic webs: A case study on holothurians. *Marine*  
439 *Pollution Bulletin* 135, 376-385.

440

441 Ruby, M.V., Davis, A., Kempton, J.H., Drexler, J.W., Bergstrom, P.D. 1992. Lead  
442 bioavailability: dissolution kinetics under simulated gastric conditions. *Environmental*  
443 *Science and Technology* 26, 1242–1248.

444

445 Setala, O., Norkko, J., Lehtiniemi, M., 2016. Feeding type affects microplastic  
446 ingestion in a coastal invertebrate community. *Marine Pollution Bulletin* 102, 95-101.

447

448 Shaw, E.J., Turner, A., 2019. Recycled electronic plastic and marine litter. *Science of*  
449 *the Total Environment* 694, 133644.

450

451 Sundar, S., Chakravarty, J., 2010. Antimony toxicity. International Journal of  
452 Environmental Research and Public Health 7, 4267-4277.  
453

454 Tamás, M.J., 2016. Cellular and molecular mechanisms of antimony transport,  
455 toxicity nad resistance. Environmental Chemistry 13, 955-962.  
456

457 Town, R.M., van Leeuwen, H.P., Blust, R., 2018. Biochemodynamic features of metal  
458 ions bound by micro- and nano-plastics in aquatic media. Frontiers in Chemistry  
459 <https://doi.org/10.3389/fchem.2018.00627>  
460

461 Tschan, M., Robinson, B., Johnson, C.A., Burgi, A., Schulin, R.D., 2010.  
462 Antimony uptake and toxicity in sunflower and maize growing in Sb-III and Sb-V  
463 contaminated soil. Plant and Soil 334, 235-245.  
464

465 Turner, A., 2018. Mobilisation kinetics of hazardous elements in marine plastics  
466 subject to an avian physiologically-based extraction test. Environmental Pollution  
467 236, 1020-1026.  
468

469 Turner, A., 2019. Trace elements in laundry dryer lint: A proxy for household  
470 contamination and discharges to waste water. Science of the Total Environment 665,  
471 568-573.  
472

473 Turner, A., Filella, M., 2017. Field-portable-XRF reveals the ubiquity of antimony in  
474 plastic consumer products. Science of the Total Environment 584-585, 982-989.  
475

476 Turner, A., Wallerstein, C., Arnold, R., 2019. Identification, origin and characteristics  
477 of bio-bead microplastics from beaches in western Europe. Science of the Total  
478 Environment 664, 938-947.  
479

480 Van Cauwenberghe, L., Claessens, M., Vandegehuchte, M.B., Janssen, C.R., 2015.  
481 Microplastics are taken up by mussels (*Mytilus edulis*) and lugworms (*Arenicola*  
482 *marina*) living in natural habitats. Environmental Pollution 199, 10-17.  
483



484 Voparil, I.M., Mayer, L.M., 2004. Commercially available chemicals that mimic a  
485 deposit feeder's (*Arenicola marina*) digestive solubilization of lipids. Environmental  
486 Science and Technology 38, 4334-4339.  
487

488 Wang, J., Wang, M.X., Ru, S.G., Liu, X.S., 2019. High levels of microplastic  
489 pollution in the sediments and benthic organisms of the South Yellow Sea, China.  
490 Science of the Total Environment 651, 1661-1669.  
491

492 Westerhoff, P., Prapaipong, P., Shock, E., Hillaireau, A., 2008. Antimony leaching  
493 from polyethylene terephthalate (PET) plastic used for bottled drinking water. Water  
494 Research 42, 551–556.  
495

496 Weston, D.P., Mayer, L.M., 1998. Comparison of in vitro digestive fluid extraction  
497 and traditional in vivo approaches as measures of polycyclic aromatic hydrocarbon  
498 bioavailability from sediments. Environmental Toxicology and Chemistry 17, 830-  
499 840.  
500

501 World Health Organization. 2003. Antimony in drinking-water. Background  
502 document for preparation of WHO Guidelines for drinking-water quality. WHO/SDE/  
503 WSH/03.04/74, Geneva.  
504

505 Yang, J.L., 2014. Comparative acute toxicity of gallium(III), antimony(III),  
506 indium(III), cadmium(II), and copper (II) on freshwater swamp shrimp  
507 (*Macrobrachium nipponense*). Biological Research 47, 13 doi: 10.1186/0717-6287-  
508 47-13  
509

510 Yang, J.L., Chen, L.H., 2018. Toxicity of antimony, gallium, and indium toward a  
511 teleost model and a native fish species of semiconductor manufacturing districts of  
512 Taiwan. Journal of Elementology 23, 191-199.  
513

514 Yellishetty, M., Huston, D., Graedel, T.E., Werner, T.T., Reck, B.K., Mudd, G.M.,  
515 2017. Quantifying the potential for recoverable resources of gallium, germanium and  
516 antimony as companion metals in Australia. Ore Geology Reviews 82, 148-159.  
517

518 Yu, X.B., Ladewig, S., Bao, S.W., Toline, C.A., Whitmire, S., Chow, A.T., 2018.  
519 Occurrence and distribution of microplastics at selected coastal sites along the  
520 southeastern United States. *Science of the Total Environment* 613, 298-305.  
521  
522 Zeng, Y.F., Li, J.X., Cao, W., Liu, X.H., Jiang, F.H., Ding, J.F., Yin, X.F., Sun, C.J.,  
523 2019. Distribution characteristics of microplastics in the seawater and sediment: A  
524 case study in Jiaozhou Bay, China. *Science of the Total Environment* 674, 27-35.

525 Table 1: Characteristics of the plastic samples employed in the experiments. Total Sb concentrations are reported as the mean and one standard  
 526 deviation arising from three XRF measurements.  
 527

sample description	polymer	Sb, $\mu\text{g g}^{-1}$	Sb origin
clear water bottle	polyethylene terephthalate (PET)	365 $\pm$ 66.6	catalytic residue
black Xmas bauble	polystyrene (PS)	890 $\pm$ 29.6	flame-retardant synergist (recycled)
white beached litter fragment	polyvinyl chloride (PVC)	6260 $\pm$ 14.7	flame-retardant synergist
white electrical casing	polycarbonate (PC)	27800 $\pm$ 100	flame-retardant synergist
yellow-green Lego brick	acrylonitrile butadiene styrene (ABS)	256 $\pm$ 23.9	colour pigment
black beached industrial biobead	polyethylene (PE)	2170 $\pm$ 30.1	flame-retardant synergist (recycled)
black rubber	rubber (R)*	47600 $\pm$ 321	flame-retardant synergist

528  
 529 \*FTIR failed to determine the precise nature of the rubber because of the high absorbance of the material.

530  
 531  
 532  
 533  
 534  
 535

536 Table 2: Concentrations of geochemically important metals, total Sb and organic  
 537 matter (as loss on ignition, LOI) in the sieved estuarine sediment sample.  
 538 Concentrations of metals and Sb are totals recovered by aqua regia and are shown as  
 539 the mean and one standard deviation arising from three independent determinations.

Al, mg g <sup>-1</sup>	6.75±0.36
Ca, mg g <sup>-1</sup>	82.2±8.9
Fe, mg g <sup>-1</sup>	14.4±0.7
Mn, µg g <sup>-1</sup>	290±11
Sb, µg g <sup>-1</sup>	0.18±0.04
LOI, %	1.44

540

541

542 Table 3: Total concentrations of Sb in the sediment amended by the different  
 543 micronized plastics (as defined in Table 1).

544

545

plastic-amended sediment	Sb, µg g <sup>-1</sup>
sediment	0.18
sediment + PET	5.1
sediment + PS	12.2
sediment + PVC	84.8
sediment + PC	376
sediment + ABS	3.6
sediment + PE	36.8
sediment + R	643

546

547

548 Table 4: Equilibrium or maximum concentrations of Sb in the time-courses shown in  
 549 Figure 1. Rate constants were derived from equilibrium concentrations by linear  
 550 regression analysis according to equation 1, and values are not shown where  
 551 regressions were non-significant ( $p > 0.05$ ).

552

553

554

555

556

557

558

sample	constant	SW	SW+BSA	SW+TA	SW+BSA+TA
sediment	$[Sb]_e$ (or $[Sb]_{max}$ ), $\mu\text{g g}^{-1}$	(0.0048)	0.0016	(0.0012)	(0.0044)
	$k$ , $(\mu\text{g g}^{-1})^{-1} \text{min}^{-1}$		8.88		
	$r^2$		0.655		
sediment + PET	$[Sb]_e$ (or $[Sb]_{max}$ ), $\mu\text{g g}^{-1}$	0.0029	(0.0013)	(0.0013)	(0.0037)
	$k$ , $(\mu\text{g g}^{-1})^{-1} \text{min}^{-1}$	4.36			
	$r^2$	0.504			
sediment + PS	$[Sb]_e$ (or $[Sb]_{max}$ ), $\mu\text{g g}^{-1}$	0.0043	0.0024	(0.0013)	0.0040
	$k$ , $(\mu\text{g g}^{-1})^{-1} \text{min}^{-1}$	6.58	2.78		44.6
	$r^2$	0.688	0.634		0.857
sediment + PVC	$[Sb]_e$ , $\mu\text{g g}^{-1}$	0.013	0.0095	0.014	0.022
	$k$ , $(\mu\text{g g}^{-1})^{-1} \text{min}^{-1}$	1.18	7.99	10.8	9.25
	$r^2$	0.846	0.774	0.807	0.777
sediment + PC	$[Sb]_e$ , $\mu\text{g g}^{-1}$	0.020	0.011	0.035	0.025
	$k$ , $(\mu\text{g g}^{-1})^{-1} \text{min}^{-1}$	0.240	2.43	0.908	0.917
	$r^2$	0.731	0.814	0.840	0.827
sediment + ABS	$[Sb]_e$ (or $[Sb]_{max}$ ), $\mu\text{g g}^{-1}$	0.026	0.036	0.036	(0.055)
	$k$ , $(\mu\text{g g}^{-1})^{-1} \text{min}^{-1}$	1.54	0.74	3.19	
	$r^2$	0.379	0.692	0.887	
sediment + PE	$[Sb]_e$ (or $[Sb]_{max}$ ), $\mu\text{g g}^{-1}$	0.0019	(1.30)	(0.015)	0.012
	$k$ , $(\mu\text{g g}^{-1})^{-1} \text{min}^{-1}$	2.87			4.25
	$r^2$	0.760			0.791
sediment + R	$[Sb]_e$ (or $[Sb]_{max}$ ), $\mu\text{g g}^{-1}$	1.65	(2.11)	0.13	(0.17)
	$k$ , $(\mu\text{g g}^{-1})^{-1} \text{min}^{-1}$	0.0216		0.132	
	$r^2$	0.933		0.882	

559

560 Table 5: Percentage bioaccessibilities of Sb in sediment amended by different  
 561 microplastics derived from equilibrium or maximum concentrations reported in Table  
 562 4 relative to total concentrations given in Table 3.

563

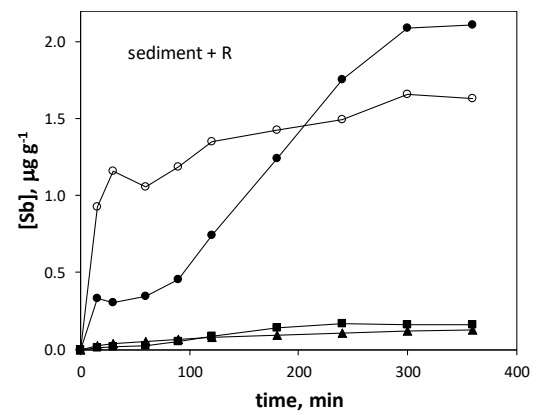
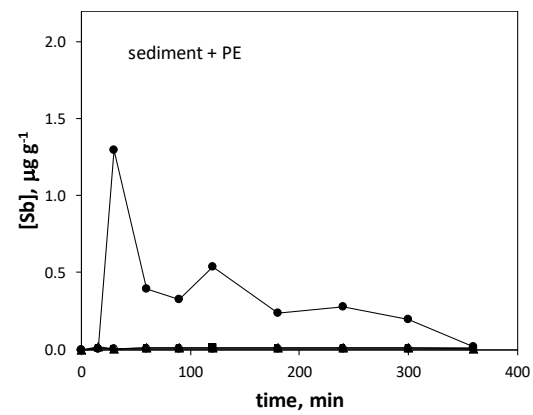
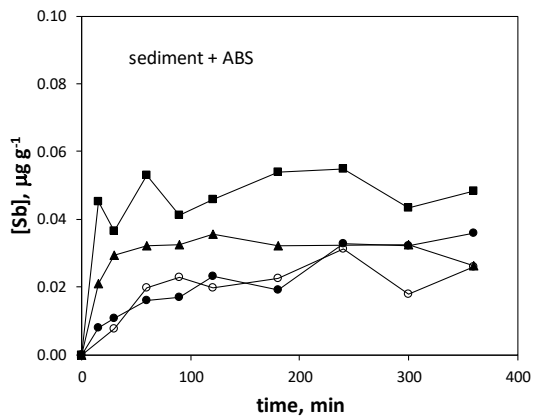
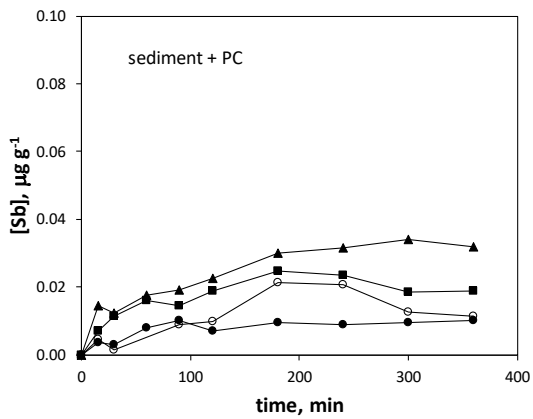
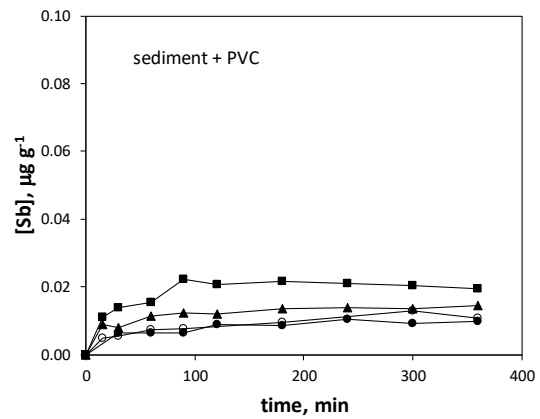
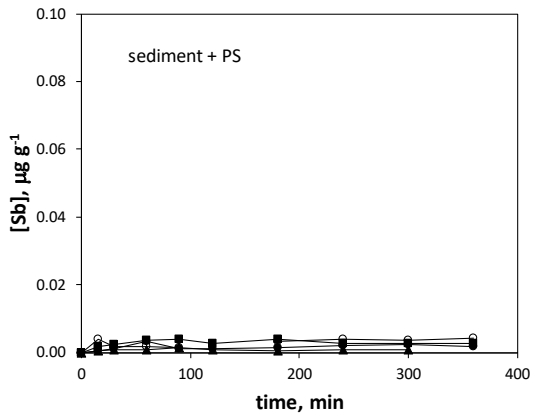
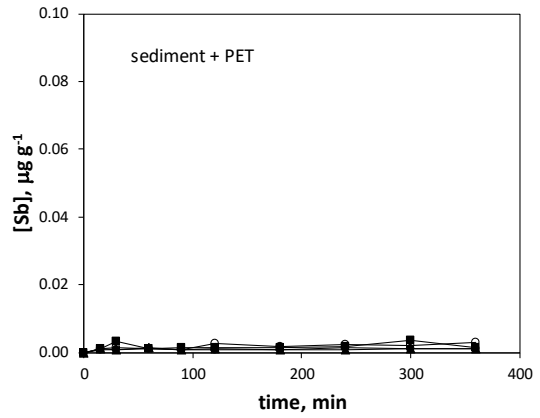
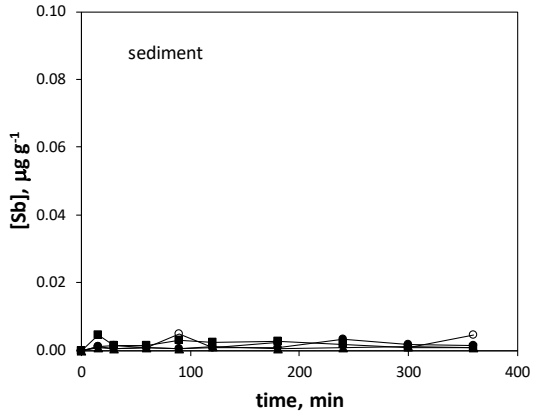
564

	SW	SW+BSA	SW+TA	SW+BSA+TA
sediment	2.67	0.89	0.67	2.44
sediment + PET	0.057	0.025	0.025	0.073
sediment + PS	0.035	0.020	0.011	0.033
sediment + PVC	0.015	0.011	0.017	0.026
sediment + PC	0.005	0.003	0.009	0.007
sediment + ABS	0.72	1.00	1.00	1.53
sediment + PE	0.005	3.53	0.041	0.033
sediment + R	0.26	0.33	0.020	0.026

565

566

567 Figure 1: Concentrations of Sb released from 25 g of wet estuarine sediment (or 18.26 g on a dry  
568 weight basis) and 25 g of wet sediment amended with 250 mg of different plastics by seawater (○) and  
569 by seawater in the presence of BSA (●), taurocholic acid (▲) and BSA plus taurocholic acid (■) as a  
570 function of time.



571

572

573



574

575

576

577

578

579

580

581

582

583

584

585

586